A field theoretical model for quarkyonic matter

Gaoqing Cao*

School of Physics and Astronomy, Sun Yat-sen University, Guangzhou 510275, China.

Jinfeng Liao†

Physics Department and Center for Exploration of Energy and Matter,
Indiana University, 2401 N Milo B. Sampson Lane, Bloomington, Indiana 47408, USA.

(Dated: July 7, 2020)

The possibility that nuclear matter at a density relevant to the interior of massive neutron stars may be a quarkyonic matter has attracted considerable recent interest. In this work, we construct a field theoretical model to describe the quarkyonic matter, that would allow quantitative and systematic calculations of its various properties. This is implemented by synthesizing the Walecka model together with the quark-meson model, where both quark and nucleon degrees of freedom are present based on the quarkyonic scenario. With this model we compute at mean-field level the thermodynamic properties of the symmetric nuclear matter and calibrate model parameters through well-known nuclear physics measurements. We find this model gives a very good description of the symmetric nuclear matter from moderate to high baryon density and demonstrates a continuous transition from nucleon-dominance to quark-dominance for the system.

PACS numbers: 11.30.Qc, 05.30.Fk, 11.30.Hv, 12.20.Ds

I. INTRODUCTION

To understand the phases and properties of strong interaction matter at high baryon density, especially in the region relevant to the interior of massive neutron stars, is a very active frontier in the research field of nuclear physics and nuclear astrophysics. The study of high baryon density region is also very relevant to ongoing experimental measurements (e.g. STAR at RHIC and HADES at SPS) of heavy ion collisions at low beam energy as well as planned programs at future facilities like the FAIR, NICA and HIAF. Both neutron star observations and heavy ion experiments will help promote our understanding of the phase diagram over a broad range of temperature and baryon density for the strong interaction matter governed by Quantum Chromodynamics (QCD). For recent reviews, see e.g. [1–5].

While a lot has been learned about the QCD matter properties at zero or very small baryon density, the high density region remains a significant challenge. There are several interesting proposals about possible phases of high density QCD matter, such as (two-flavor) color superconductivity [6, 7], color-flavor locking [8], or quarkyonic matter [9]. In the density region comparable with the neutron star interior, the quarkyonic matter might be more directly relevant, thus we shall focus on that phase in this work. The quarkyonic matter was first proposed by following insights from the large N_c analysis and emphasizing the coexistence of nucleon/quark degrees of freedom [9–12]. In the large isospin density (but small baryon density) region, an analogous "quarksonic matter" was proposed by following similar arguments in

Ref. [13]. Recently, there has been increasing interest to explore the possible existence of quarkyonic matter inside compact stars and the consequences for relevant astrophysical observations [14–21].

Certain issues require improvements over previous studies, many of which were based on simple (and often oversimplified) picture implementations with crude and ad hoc approximations. The chiral symmetry restoration with increasing density often lacked a dynamical treatment. The important physics constraints from the lower density side, e.g. nuclear matter saturation properties, were not carefully checked. Given these issues, it is therefore important to develop a more sophisticated field theoretical model to study the quarkyonic matter – one that would allow systematic calculations of various properties and quantitative scrutiny of important physics constraints. This is the main goal of our study, with the first successful step to be reported in the present paper. The rest of paper is organized as follows. In Sec.II, the model Lagrangian density is constructed and the main formalism is developed in great details by focusing on symmetric nuclear matter. Then in Sec.III, the model parameters are fixed according to the saturation properties observed from low energy nuclear experiments. In Sec.IV, the thermodynamic properties are computed for quarkyonic matter for a wide range of baryon densities within our new model. Finally, we conclude in Sec.V.

II. AN EFFECTIVE MODEL FOR QUARKYONIC MATTER

A. Lagrangian and thermodynamic potential

By following the spirit of quark-baryonic (or quarkyonic) matter (QBM) with both quarks and baryons as

the effective degrees of freedom of the strong interaction system, we construct a field theoretical model which combines the quark-meson (QM) model [22] together with the well-known Walecka model [23]. The quark-meson and Walecka models are common on one aspect:

mesons are the "messengers" of the interactions between quarks or baryons. The overall Lagrangian density of our two-flavor model is composed of three parts, that is, $\mathcal{L}_{QBM} \equiv \mathcal{L}_{\mathrm{q}} + \mathcal{L}_{\mathrm{N}} + \mathcal{L}_{\mathrm{M}}$ with the following explicit forms:

$$
\mathcal{L}_{\mathrm{q}} = \bar{q}\Big[i\slashed{\partial} + \Big(\mu_B/N_c + \frac{\mu_I}{2}\tau_3\Big)\gamma^0 - g_q\left(\sigma + i\gamma^5\boldsymbol{\tau}\cdot\boldsymbol{\pi}\right)\Big]q,
$$

$$
\mathcal{L}_{\mathrm{N}} = \bar{N}\Big[i\slashed{\partial} + \Big(\mu_B + \frac{\mu_I}{2}\tau_3\Big)\gamma^0 - g_{\mathrm{Ns}}\left(\sigma + i\gamma^5\boldsymbol{\tau}\cdot\boldsymbol{\pi}\right) + g_{\mathrm{Nv}}\left(\slashed{\rho} - \gamma^5\slashed{A}\right)\cdot\tau\Big]N,
$$

$$
\mathcal{L}_{\mathrm{M}} = \frac{1}{2}\left(\partial_\mu\sigma\partial^\mu\sigma + D_\mu\boldsymbol{\pi}\cdot D^\mu\boldsymbol{\pi}\right) - \frac{\lambda}{4}\left(\sigma^2 + \boldsymbol{\pi}\cdot\boldsymbol{\pi} - v^2\right)^2 + c\,\sigma + \frac{1}{2}g_{\mathrm{sv}}\left(\sigma^2 + \boldsymbol{\pi}\cdot\boldsymbol{\pi}\right)\left(\rho_\mu\cdot\rho^\mu + A_\mu\cdot A^\mu\right)
$$

$$
- \frac{1}{4}\left(D_\mu\rho_\nu - D_\nu\rho_\mu\right)\cdot\left(D^\mu\rho^\nu - D^\nu\rho^\mu\right) + \frac{1}{2}m_v^2\rho_\mu\cdot\rho^\mu - \frac{1}{4}\left(D_\mu A_\nu - D_\nu A_\mu\right)\cdot\left(D^\mu A^\nu - D^\nu A^\mu\right) + \frac{1}{2}m_a^2 A_\mu\cdot A^\mu \ . \quad (1)
$$

Here, the quantum fields are defined as the following: $q(x) = (u(x), d(x))^T$ denotes the two-flavor quark field with color degrees of freedom $N_c = 3$, $N(x) = (p(x), n(x))^T$ is the two-flavor nucleon field *outside* the Fermi spheres of quarks if exist, $\sigma(x)$ and $\boldsymbol{\pi}(x)$ are the scalar and pseudoscalar mesons, while ρ_μ^a (with ρ_μ^0 the ω meson) and A_μ^a ($a = 0, \ldots, 3$) are vector and axial vector mesons, respectively. The baryon and isospin chemical potentials are given by μ_B and $\frac{\mu_I}{2}$, respectively. The isospin matrices are

$$
\tau = \left(1, \frac{\tau_x - i\tau_y}{\sqrt{2}}, \frac{\tau_x + i\tau_y}{\sqrt{2}}, \tau_z\right)
$$

with τ_x, τ_y and τ_z the Pauli matrices in flavor space. The derivative operators are defined as $D_0 = \partial_0 \mp i\mu_I$ for the charged $\pi^\pm, \rho_\mu^\pm$ and $A_\mu^\pm$, and $D_\mu = \partial_\mu$ for the others. For the isospin symmetric case with $\mu_I = 0$, the Lagrangian has exact chiral symmetry in the chiral limit $c = 0$ and when chiral anomaly is neglected by choosing $m_v = m_a$. In the realistic case, with the linear coefficient $c \neq 0$ and the masses $m_v < m_a$, there is only approximate chiral symmetry in the QBM model.

Let us first discuss the vacuum of the above model at temperature $T = 0$ and chemical potential $\mu = 0$. In mean field approximation, the thermodynamic potential is only given by the mesonic part in the vacuum, that is,

$$
\Omega_v = \frac{\lambda}{4}\left(\langle\sigma\rangle^2 + \langle\boldsymbol{\pi}\rangle\cdot\langle\boldsymbol{\pi}\rangle - v^2\right)^2 - c\langle\sigma\rangle, \quad (2)
$$

the global minimum of which locates at $\langle\boldsymbol{\pi}\rangle = 0$ and

$$
\langle\sigma\rangle = \sum_{t=\pm}\left[\frac{c}{2\lambda} + t\,i\sqrt{\frac{v^6}{27} - \left(\frac{c}{2\lambda}\right)^2}\right]^{1/3}. \quad (3)
$$

It can be checked that we simply have $\langle\sigma\rangle = v$ in the chiral limit $c \to 0$. Based on the ground state, the sigma and pion masses can then be derived as [22]

$$
m_\sigma^2 = \lambda\left(3\langle\sigma\rangle^2 - v^2\right), \ m_\pi^2 = \lambda\left(\langle\sigma\rangle^2 - v^2\right), \quad (4)
$$

which indicate the σ and π mesons as the massive and Goldstone modes, respectively.

If we adopt the quark version of Goldberger-Treiman relation: $f_\pi^2 g_q^2 = m_{\mathrm{q}}^2$ [24], the expectation value of σ is found to be $\langle\sigma\rangle_v = f_\pi$ in vacuum. Then, the parameters in the mesonic sector can be determined by the vacuum masses m_σ, m_π and pion decay constant f_π as

$$
\lambda = \frac{m_\sigma^2 - m_\pi^2}{2f_\pi^2}, \ v^2 = \frac{m_\sigma^2 - 3m_\pi^2}{m_\sigma^2 - m_\pi^2}f_\pi^2, \ c = f_\pi m_\pi^2. \quad (5)
$$

We next discuss the other model parameters in the quark and baryonic sectors. Firstly, the coupling constants between the scalar sector mesons and quarks or nucleons can be fixed by their vacuum masses as $g_{\mathrm{q}} = m_{\mathrm{q}}^v/f_\pi \equiv m_\sigma/(2f_\pi)$ [22] and $g_{\mathrm{Ns}} = m_{\mathrm{N}}^v/f_\pi$. The quantities m_π, f_π and m_{N}^v are well determined from the experiments. The other parameters like m_{q}^v (or m_σ), g_{Nv} and g_{sv} will be constrained later by the empirical saturation properties of nuclear matter. Note also that with the additional scalar-vector interaction, the vector mass is given by $m_{\mathrm{v}}^2 + g_{\mathrm{sv}}f_\pi^2 = (785 \text{ MeV})^2$ in the vacuum.

We now turn to compute thermodynamics at finite temperature and chemical potentials, where quarks and nucleons will also give contributions. In this paper, we will focus on the (isospin-)symmetric nuclear matter as a first step, by choosing $\mu_B > 0$ and $\mu_I = 0$. The thermodynamic contributions from the quark and baryon sectors are given below:

$$\Omega_q^t = -4N_cT\sum_{t=\pm}\int \frac{d^3p}{(2\pi)^3}\ \ln\left(1+e^{-\left[E_{\mathrm{q}}(\mathbf{p})+t\frac{\mu_B}{N_c}\right]/T}\right), \tag{6}$$

$$\Omega_N^t = -\frac{1}{2}\left(g_{\mathrm{sv}}\langle\sigma\rangle^2+m_{\mathrm{v}}^2\right)\left(\langle\omega_0\rangle^2+(\langle\rho_0^3\rangle)^2\right) - 4T\sum_{t=\pm}\int \frac{d^3p}{(2\pi)^3}\ \ln\left(\frac{1+e^{-[E_{\mathrm{N}}(\mathbf{p})+t(\mu_B-g_{\mathrm{Nv}}\langle\omega_0\rangle)]/T}}{1+e^{-[E_{\mathrm{N}}(\mathbf{p})+t(\mu_B'-g_{\mathrm{Nv}}\langle\omega_0\rangle)]/T}}\right), \tag{7}$$

where the dispersion relations are $E_{\mathrm{q}}(\mathbf{p}) = \left(\mathbf{p}^2+m_{\mathrm{q}}^2\right)^{1/2}$ with $m_{\mathrm{q}} = g_{\mathrm{q}}\langle\sigma\rangle$ and $E_{\mathrm{N}}(\mathbf{p}) = \left(\mathbf{p}^2+m_{\mathrm{N}}^2\right)^{1/2}$ with $m_{\mathrm{N}} = g_{\mathrm{Ns}}\langle\sigma\rangle$. The vector mean-field condensate is subject to the physical constraint $0 \leq g_{\mathrm{Nv}}\langle\omega_0\rangle \leq \mu_B$, that is, the nucleon chemical potential is reduced by $\langle\omega_0\rangle$ but never changes sign.

The crucial step here is to implement the quarkyonic picture in the momentum space, in which the interior of the Fermi sea is filled up by quarks while the nucleons are excluded to reside in an outside shell of the Fermi sea [9, 10]. In our model, the boundary for "Pauli-blocked" nucleon sphere is characterized by an effective chemical potential μ_B'. The nucleons in the quarkyonic matter exist between the Fermi sphere stretched by μ_B' and μ_B. As one can tell in Ω_N^t: the thermodynamics potential of the nucleonic part is obtained by subtracting the supposed inner contribution (with μ_B') out of the naive total one (with μ_B). It is important to have an appropriate scheme for determining the μ_B'. One possible choice is the μ_B-linear form:

$$\mu_B' = \mu_B - (N_c m_{\mathrm{q}} - m_{\mathrm{N}}), \tag{8}$$

based on comparing kinetic energy of a baryon with that of N_c quarks. Another nonlinear choice assumes that the momenta of the valence quarks of proton (uud) and neutron (udd) are the same and nucleons are blocked by the free quarks from the Fermi sphere [15], that is,

$$\mu_B' = \sqrt{m_{\mathrm{N}}^2+(N_c k_F)^2}, \tag{9}$$

which is smaller than μ_B as $N_c m_{\mathrm{q}} > m_{\mathrm{N}}$. Here, the effective Fermi momentum of the u and d quarks is

$$k_F = \left[(\mu_B/N_c)^2-m_{\mathrm{q}}^2\right]^{1/2}. \tag{10}$$

This definition is based on comparing momentum of a baryon with that of N_c quarks. We will perform computations with both choices of μ_B' and compare their results later.

B. Gap equations and energy density

In mean field approximation, the total thermodynamic potential is then $\Omega = \Omega_v+\Omega_q^t+\Omega_N^t$ and the gap equations can be obtained from the extremal conditions $\partial\Omega/\partial X = 0$ $(X = \langle\omega_0\rangle, \langle\sigma\rangle)$ as

$$\langle\omega_0\rangle = -4\sum_{t=\pm}\int \frac{d^3p}{(2\pi)^3}\frac{t\frac{g_{\mathrm{Nv}}}{m_{\mathrm{v}}^2+g_{\mathrm{sv}}\langle\sigma\rangle^2}}{1+e^{[E_{\mathrm{N}}(\mathbf{p})+t(\mu_B-g_{\mathrm{Nv}}\langle\omega_0\rangle)]/T}} + 4\sum_{t=\pm}\int \frac{d^3p}{(2\pi)^3}\frac{t\frac{g_{\mathrm{Nv}}}{m_{\mathrm{v}}^2+g_{\mathrm{sv}}\langle\sigma\rangle^2}}{1+e^{[E_{\mathrm{N}}(\mathbf{p})+t(\mu_B'-g_{\mathrm{Nv}}\langle\omega_0\rangle)]/T}}, \tag{11}$$

$$\lambda\left(\langle\sigma\rangle^2-v^2\right)\langle\sigma\rangle - c - g_{\mathrm{sv}}\langle\sigma\rangle\langle\omega_0\rangle^2 + 4N_c\sum_{t=\pm}\int \frac{d^3p}{(2\pi)^3}\frac{g_{\mathrm{q}}m_{\mathrm{q}}/E_{\mathrm{q}}(\mathbf{p})}{1+e^{[E_{\mathrm{q}}(\mathbf{p})+t\frac{\mu_B}{N_c}]/T}} + 4\sum_{t=\pm}\int \frac{d^3p}{(2\pi)^3}\frac{g_{\mathrm{Ns}}m_{\mathrm{N}}/E_{\mathrm{N}}(\mathbf{p})}{1+e^{[E_{\mathrm{N}}(\mathbf{p})+t(\mu_B-g_{\mathrm{Nv}}\langle\omega_0\rangle)]/T}}$$

$$-4\sum_{t=\pm}\int \frac{d^3p}{(2\pi)^3}\frac{g_{\mathrm{Ns}}m_{\mathrm{N}}/E_{\mathrm{N}}(\mathbf{p})+t\,\partial\mu_B'/\partial\langle\sigma\rangle}{1+e^{[E_{\mathrm{N}}(\mathbf{p})+t(\mu_B'-g_{\mathrm{Nv}}\langle\omega_0\rangle)]/T}} = 0, \tag{12}$$

where the derivatives of the effective chemical potential are $\frac{\partial\mu_B'}{\partial\langle\sigma\rangle} = g_{\mathrm{Ns}} - g_{\mathrm{q}}N_c$ for the linear choice and $\frac{\partial\mu_B'}{\partial\langle\sigma\rangle} = \frac{1}{\mu_B'}\left[g_{\mathrm{Ns}}m_{\mathrm{N}} - g_{\mathrm{q}}N_c^2m_{\mathrm{q}}\right]$ for the nonlinear choice, respectively.

Furthermore, the baryon number and entropy densities can be derived directly according to the thermodynamic relationships $n_B = -\partial\Omega/\partial\mu_B$ and $s = -\partial\Omega/\partial T$ as:

$$n_B = -4\sum_{t=\pm}\int \frac{d^3p}{(2\pi)^3}t\left(\frac{1}{1+e^{[E_{\mathrm{q}}(\mathbf{p})+t\frac{\mu_B}{N_c}]/T}} + \frac{1}{1+e^{[E_{\mathrm{N}}(\mathbf{p})+t(\mu_B-g_{\mathrm{Nv}}\langle\omega_0\rangle)]/T}} - \frac{\partial\mu_B'/\partial\mu_B}{1+e^{[E_{\mathrm{N}}(\mathbf{p})+t(\mu_B'-g_{\mathrm{Nv}}\langle\omega_0\rangle)]/T}}\right), \tag{13}$$

$$s = 4\sum_{t=\pm}\int \frac{d^3p}{(2\pi)^3}\left(N_c\ln\left(1+e^{-[E_{\mathrm{q}}(\mathbf{p})+t\frac{\mu_B}{N_c}]/T}\right) + \frac{N_c E_{\mathrm{q}}(\mathbf{p})+t\,\mu_B}{T\left(1+e^{[E_{\mathrm{q}}(\mathbf{p})+t\frac{\mu_B}{N_c}]/T}\right)} + \ln\left(1+e^{-[E_{\mathrm{N}}(\mathbf{p})+t(\mu_B-g_{\mathrm{Nv}}\langle\omega_0\rangle)]/T}\right) + \right.$$

$$\left. \frac{E_{\mathrm{N}}(\mathbf{p})+t(\mu_B-g_{\mathrm{Nv}}\langle\omega_0\rangle)}{T\left(1+e^{[E_{\mathrm{N}}(\mathbf{p})+t(\mu_B-g_{\mathrm{Nv}}\langle\omega_0\rangle)]/T}\right)} - \ln\left(1+e^{-[E_{\mathrm{N}}(\mathbf{p})+t(\mu_B'-g_{\mathrm{Nv}}\langle\omega_0\rangle)]/T}\right) - \frac{E_{\mathrm{N}}(\mathbf{p})+t(\mu_B'-g_{\mathrm{Nv}}\langle\omega_0\rangle)}{T\left(1+e^{[E_{\mathrm{N}}(\mathbf{p})+t(\mu_B'-g_{\mathrm{Nv}}\langle\omega_0\rangle)]/T}\right)}\right), \tag{14}$$

where the explicit forms of the derivatives of the effective chemical potentials in Eq.(13) are given by $\frac{\partial \mu'_B}{\partial \mu_B} = 1$ for the linear choice and $\frac{\partial \mu'_B}{\partial \mu_B} = \frac{\mu_B}{\mu'_B}$ for the nonlinear choice, respectively. Thus, the energy density of the quarkyonic matter is found to be

$$
\begin{aligned}
\epsilon &\equiv \Omega + \mu_B n_B + sT - (T = \mu_B = 0) \\
&= \frac{\lambda}{4}\left(\langle\sigma\rangle^2 - v^2\right)^2 - c\,\langle\sigma\rangle - \frac{1}{2}(m_v^2 + g_{sv}\langle\sigma\rangle^2)\langle\omega_0\rangle^2 + 4\sum_{t=\pm}\int \frac{d^3p}{(2\pi)^3}\left(\frac{N_c E_q(\mathbf{p})}{1+e^{[E_q(\mathbf{p})+t\frac{\mu_B}{N_c}]/T}} + \frac{E_N(\mathbf{p})-t\,g_{Nv}\langle\omega_0\rangle}{1+e^{[E_N(\mathbf{p})+t(\mu_B-g_{Nv}\langle\omega_0\rangle)]/T}}\right. \\
&\qquad \left. -\frac{E_N(\mathbf{p})+t\left[(\mu'_B - \mu_B \partial\mu'_B/\partial\mu_B) - g_{Nv}\langle\omega_0\rangle\right]}{1+e^{[E_N(\mathbf{p})+t(\mu'_B-g_{Nv}\langle\omega_0\rangle)]/T}}\right) - (T = \mu_B = 0), \quad (15)
\end{aligned}
$$

where we assume $m_N^2 + (N_c k_F)^2 > 0$ and the vacuum term is excluded to make sure the medium energy vanishes in the vacuum.

To fix the remaining parameters of the model, we turn to zero temperature limit where some empirical results are well known. The explicit form of the baryon density Eq.(13) for the quarkyonic matter becomes

$$
n_B = n_B^q + n_B^N - n_B^{N'} \equiv \frac{2p_{qF}^3}{3\pi^2} + \frac{2p_{NF}^3}{3\pi^2} - \frac{\partial\mu'_B}{\partial\mu_B}\frac{2p_{N'F}^3}{3\pi^2}, \quad (16)
$$

where p_{NF} and $p_{N'F}$ are the Fermi momenta of the occupied and Pauli-blocked nucleon states, and p_{qF} is the Fermi momentum of the occupied quark states, respectively. The Fermi momenta are related to the chemical potentials through the Fermi energies as

$$
E_{qF} \equiv E_q(p_{qF}) = \mu_B/N_c, \;\; E_{NF} \equiv E_N(p_{NF}) = \mu_B - g_{Nv}\langle\omega_0\rangle, \;\; E_{N'F} \equiv E_N(p_{N'F}) = \mu'_B - g_{Nv}\langle\omega_0\rangle. \quad (17)
$$

In this case, we're glad that the momentum integrations involved in the gap equations Eqs.(11) and (12) and energy density Eq.(15) can be carried out explicitely with the help of Fermi momenta as

$$
0 = \langle\omega_0\rangle(m_v^2 + g_{sv}\langle\sigma\rangle^2) - g_{Nv}\,\Delta\frac{2p_{NF}^3}{3\pi^2}, \quad (18)
$$

$$
\begin{aligned}
0 &= \lambda\left(\langle\sigma\rangle^2 - v^2\right)\langle\sigma\rangle - c - g_{sv}\langle\sigma\rangle\langle\omega_0\rangle^2 + \frac{g_{Ns}m_N}{\pi^2}\Delta\left[E_{NF}p_{NF} - m_N^2\ln\left(\frac{E_{NF}+p_{NF}}{m_N}\right)\right] \\
&\quad + N_c\frac{g_q m_q}{\pi^2}\left[E_{qF}p_{qF} - m_q^2\ln\left(\frac{E_{qF}+p_{qF}}{m_q}\right)\right] + \frac{\partial\mu'_B}{\partial\langle\sigma\rangle}\frac{2p_{N'F}^3}{3\pi^2}, \quad (19)
\end{aligned}
$$

$$
\begin{aligned}
\epsilon &= \frac{\lambda}{4}\left(\langle\sigma\rangle^2 - v^2\right)^2 - c\,\langle\sigma\rangle + \frac{1}{2}(m_v^2 + g_{sv}\langle\sigma\rangle^2)\langle\omega_0\rangle^2 + \frac{1}{4\pi^2}\Delta\left[2E_{NF}^3 p_{NF} - m_N^2 E_{NF}p_{NF} - m_N^4\ln\left(\frac{E_{NF}+p_{NF}}{m_N}\right)\right] \\
&\quad + \frac{N_c}{4\pi^2}\left[2E_{qF}^3 p_{qF} - m_q^2 E_{qF}p_{qF} - m_q^4\ln\left(\frac{E_{qF}+p_{qF}}{m_q}\right)\right] + \left(\mu'_B - \mu_B\frac{\partial\mu'_B}{\partial\mu_B}\right)\frac{2p_{N'F}^3}{3\pi^2} - (\mu_B = 0), \quad (20)
\end{aligned}
$$

where the symbol "Δ" means excluding the corresponding one with $N \to N'$ for the energy and momentum. Combining Eqs.(16) and (18), we find $\langle\omega_0\rangle(m_v^2 + g_{sv}\langle\sigma\rangle^2) = g_{Nv}\,\Delta n_B^N$ for the linear choice, which actually has a definite physical meaning: the vector condensate is proportional to the nucleon density [23].

III. MODEL PARAMETERS

From the experimental measurements associated with finite nuclei, some properties of the infinite and isospin symmetric nuclear matter were extracted: the saturation density $n_0 \approx 0.16$ fm^{-3} [25], the energy per nucleon at this density $E/N \equiv \epsilon/n_B - m_N^v = -16$ MeV [26, 27] as well as the compressibility $K_0 = 240 \pm 20$ MeV [28].

Theoretically, they are related with each other as:

$$
\left.\frac{\partial(E/N)}{\partial n_B}\right|_{n_B=n_0}^{\langle\sigma\rangle} = -\frac{\epsilon}{n_0^2} + \frac{\mu_{Bc}}{n_0} = \frac{P_c}{n_0} = 0, \quad (21)
$$

$$
K_0 = 9\left.\frac{\partial^2(E/N)}{\partial(n_B/n_0)^2}\right|_{n_B=n_0}, \quad (22)
$$

from which it is easy to infer the pressure $P_c = 0$ and the critical chemical potential $\mu_{Bc} = E/N + m_N^v = 923$ MeV.

Now, we use these saturation properties to fix the remaining parameters. The dynamical quark mass is varied in the range $m_q^v \gtrsim m_N^v/3$ which guarantees the stability of nucleons against the decay to quarks in vacuum. Then the order parameters $\langle\sigma\rangle$ and $\langle\omega_0\rangle$ and coupling constants g_{Nv} and g_{sv} are fixed by solving the gap equations Eqs.(11) and (12), saturation equation Eq.(21) and

the saturation energy $E/N = -16$ MeV self-consistently. The extracted results for g_{sv} and the associated nucleon fraction $R_N \equiv \Delta n_B^N / n_B$ as functions of m_q^v are shown together in Fig. 1 for both linear and nonlinear μ'_B choices. As we can see, the results are quantitatively consistent with each other for these choices, with only minor differences in the relatively smaller mass region.
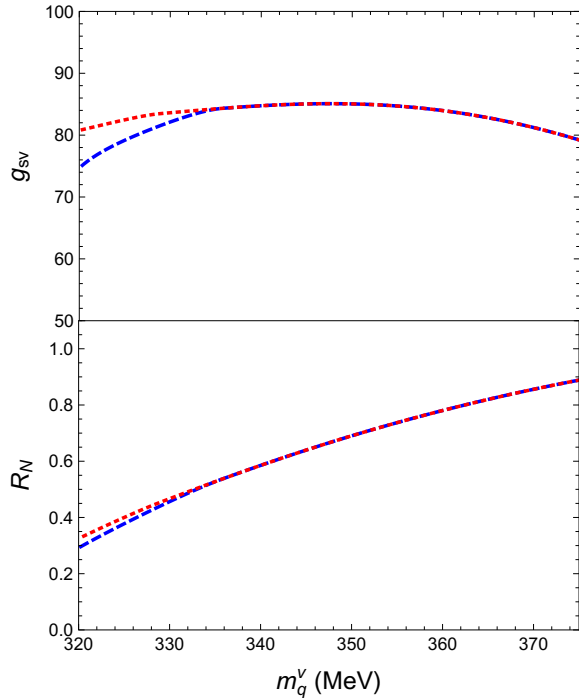

FIG. 1. The extracted values for the coupling g_{sv} and the associated nucleon fraction R_N as functions of the quark vacuum mass m_q^v for both linear (red dotted) and nonlinear (blue dashed) μ'_B choices.

In order to further fix the vacuum quark mass in our model, we show our model calculations together with the empirical constraint [28] in Fig.2 for the compressibility at saturation density n_0. From the results, we find the best agreement is achieved for $m_q^v = 370.4 \pm 0.8$ MeV. In the rest of this paper, we will then adopt the value $m_q^v = 370.4$ MeV, with the corresponding nucleon ratio $R_N \approx 85.8\%$ for both choices of μ'_B at saturation density. We note that at this density there is a nonzero albeit very small fraction of quarks that already emerge and coexist with the nucleons. The corresponding coupling constants are also fixed to be $g_{Nv} \approx 7.2$ and $g_{sv} \approx 81$, respectively.

At this point, all of our model parameters are fixed and the model satisfactorily catches the nuclear matter properties at saturation density. Lastly we examine the liquid-gas transition at this density. In Fig. 3, we show the thermodynamic potential Ω as a function of the quark condensate $\langle \sigma \rangle$ for both choices of μ'_B at the critical chemical potential μ_{Bc}. As one can see, there is a typical first-order transition structure with two degenerate minima: one at the vacuum value $\langle \sigma \rangle = f_\pi$, and the
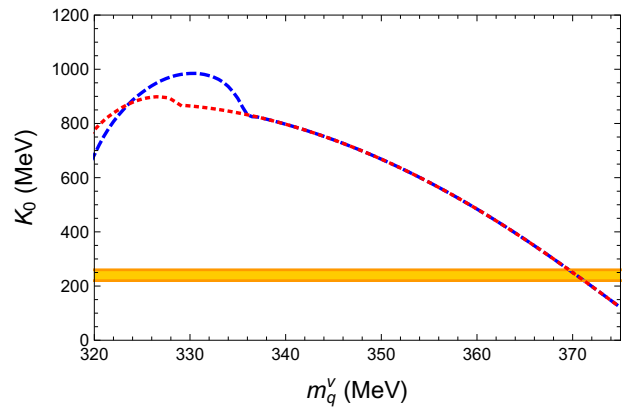

FIG. 2. The compressibility K_0 of quarkyonic matter at saturation density n_0 as a function of the quark vacuum mass m_q^v for both linear (red dotted) and nonlinear (blue dashed) μ'_B choices. The yellow band is the constraint from experiments [28].

other new one at $\langle \sigma \rangle = 69.2$ MeV. At μ_{Bc}, the chiral condensate jumps from the vacuum value to the smaller one. In the next section we will analyze the matter properties at chemical potential beyond this transition point.
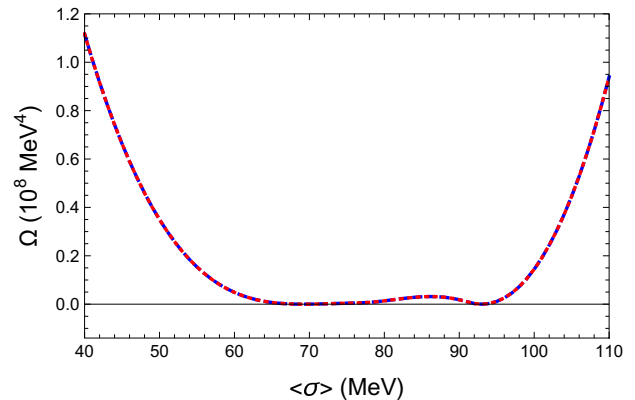

FIG. 3. The thermodynamic potential Ω as a function of the chiral condensate $\langle \sigma \rangle$ at the critical chemical potential μ_{Bc}. The conventions are the same as those in Fig.1.

IV. THE QUARKYONIC MATTER PROPERTIES

In this section we present results for quarkyonic matter properties in the region of a few times the saturation density. The chiral and vector condensates as well as the corresponding nucleon ratio are shown in Fig. 4 as functions of baryon chemical potential. We find that both $\langle \sigma \rangle$ and R_N decreas rapidly while $\langle \omega_0 \rangle$ increases with μ_B. This implies that with increasing density, the chiral symmetry gets gradually restored with the quarks becoming lighter and more abundant. The increasing of $\langle \omega_0 \rangle$ could be understood as due to the enhancement of the nucleon

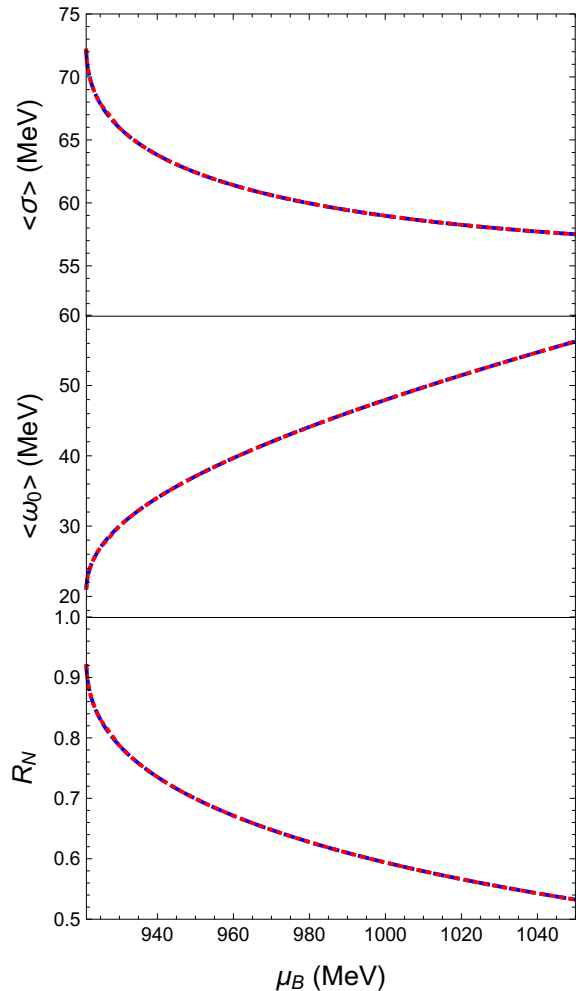density with μ_B, even though the nucleon fraction R_N decreases.

FIG. 4. The chiral condensate $\langle\sigma\rangle$, vector condensate $\langle\omega_0\rangle$ and nucleon ratio R_N as functions of chemical potential μ_B in the chiral symmetry partially restored phase. The conventions are the same as those in Fig.1.

We now compute the energy density of the system and present the closely related E/N in the upper panel of Fig. 5. As we can see, the E/N starts from the minimum value of $-16\,\mathrm{MeV}$ at the saturation density n_0 and steadily increases toward higher density. A key quantity related to the equation-of-state (EOS) for the quarkyonic matter is the speed of sound $C_v \equiv \sqrt{\frac{\partial P}{\partial \epsilon}}$ [29]. In the lower panel of Fig. 5, we show C_v^2 versus baryon density for both linear and nonlinear μ'_B choices, which show small deviation from each other. In both cases, the speed of sound increases quickly between $1 \sim 2n_0$ and then approaches the high density asymptotical limit rather smoothly, in consistency with a continuous transition feature [29]. We note that our results are consistent with those given in Ref. [15, 17] for both small and large density, except that the prominent peak structure in the intermediate density is absent in our model. The differ-

ence could be due to the hard core feature in Ref. [17] which we do not have. Actually, the monotonous feature of C_v was also found in a recent quite convincing study when diquark dynamics is ignored [30].
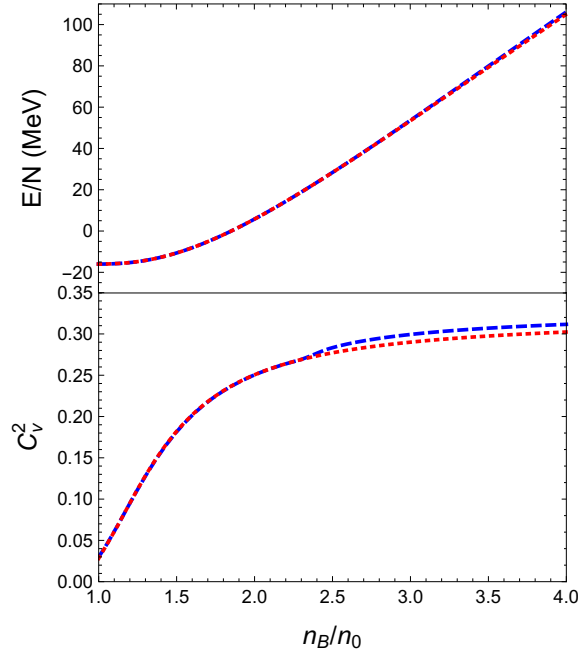

FIG. 5. The energy per nucleon E/N and speed of sound C_v^2 as functions of baryon density n_B, the range of which corresponds to that of μ_B in Fig. 4. The conventions are the same as those in Fig.1.

Finally, we proceed to compare our EOS with the experimental extraction as well as other model calculations [31], see Fig. 6. The comparison indicates that our results based on quarkyonic matter are reasonably consistent with the experimental constraints, especially in the large density region where quarks become more and more important.

V. CONCLUSIONS

In this work, we propose a field theoretical model for quarkyonic matter by combining the Walecka model together with the quark-meson model. We have systematically calibrated the model parameters based on various hadron properties in the vacuum as well as nuclear matter properties a the saturation density. Based on that, we then extend our calculations to the large baryon density region and find a number of interesting results. Firstly, the chiral symmetry is partially and smoothly restored with increasing baryon chemical potential μ_B (see the upper panel of Fig.4), contrary to the first-order transition and nearly full restoration in Nambu–Jona-Lasinio model [24]. Secondly, the vector condensate increases with μ_B (see the middle panel of Fig.4) as the nucleon density increases, which can be easily expected from the
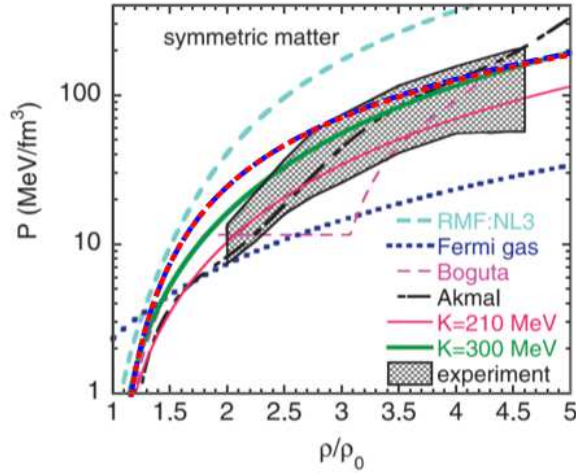
FIG. 6. The comparison between our quarkyonic matter model results with those from experimental constraints (shadow region) and other model predictions (colored lines) for the pressure P of symmetric nuclear matter as a function of baryon density. Note that this plot is made via adapting an original figure extracted from Re. [31], for which we keep the original notations of the various physical quantities. In particular, the baryon density ρ (ρ_0) in this plot corresponds to n_B (n_0) we use in other places of the paper.

proportionality shown in Eq.(18). Thirdly, the nucleon ratio reduces (see the lower panel of Fig.4) as the quark density enhances more quickly than the nucleon density, which indicates gradual dominance of the quark degrees of freedom at larger chemical potential. Finally we have calculated the equation of state and especially the speed of sound for quarkyonic matter in this model. The results are found to be consistent with predictions of various other models as well as with experimental constraints for symmetric nuclear matter at a few times the saturation density. Our overall conclusion is that, quantitative results from our field theoretical model of quarkyonic matter provide a satisfactory description about the properties of vacuum as well as nuclear matter up to several times the saturation density. Apart for the first-order liquid-gas transition at $\mu_{Bc} = 923\,\mathrm{MeV}$, the results feature a continuous transition from nucleon-dominated regime to quark-dominated one along with gradual restoration of the chiral symmetry. It will be a natural step to further explore the implications of this quarkyonic matter model for the interiors of neutron stars, such as had been done in Ref. [15]. The results shall be reported in a future publication.

[1] D. Page and S. Reddy, Ann. Rev. Nucl. Part. Sci. **56**, 327-374 (2006) doi:10.1146/annurev.nucl.56.080805.140600 [arXiv:astro-ph/0608360 [astro-ph]].

[2] J. M. Lattimer and M. Prakash, Phys. Rept. **621**, 127-164 (2016) doi:10.1016/j.physrep.2015.12.005 [arXiv:1512.07820 [astro-ph.SR]].

[3] P. Braun-Munzinger, V. Koch, T. Schfer and J. Stachel, Phys. Rept. **621**, 76-126 (2016) doi:10.1016/j.physrep.2015.12.003 [arXiv:1510.00442 [nucl-th]].

[4] A. Bzdak, S. Esumi, V. Koch, J. Liao, M. Stephanov and N. Xu, Phys. Rept. **853**, 1-87 (2020) doi:10.1016/j.physrep.2020.01.005 [arXiv:1906.00936 [nucl-th]].

[5] X. Luo and N. Xu, Nucl. Sci. Tech. **28**, no. 8, 112 (2017) doi:10.1007/s41365-017-0257-0 [arXiv:1701.02105 [nucl-ex]].

[6] M. G. Alford, K. Rajagopal and F. Wilczek, Phys. Lett. B **422**, 247 (1998) doi:10.1016/S0370-2693(98)00051-3 [hep-ph/9711395].

[7] R. Rapp, T. Schfer, E. V. Shuryak and M. Velkovsky, Phys. Rev. Lett. **81**, 53 (1998) doi:10.1103/PhysRevLett.81.53 [hep-ph/9711396].

[8] M. G. Alford, K. Rajagopal and F. Wilczek, Nucl. Phys. B **537**, 443 (1999) doi:10.1016/S0550-3213(98)00668-3 [hep-ph/9804403].

[9] L. McLerran and R. D. Pisarski, Nucl. Phys. A **796**, 83 (2007) doi:10.1016/j.nuclphysa.2007.08.013 [arXiv:0706.2191 [hep-ph]].

[10] L. McLerran, K. Redlich and C. Sasaki, Nucl. Phys. A **824**, 86-100 (2009) doi:10.1016/j.nuclphysa.2009.04.001 [arXiv:0812.3585 [hep-ph]].

[11] A. Andronic, D. Blaschke, P. Braun-Munzinger, J. Cleymans, K. Fukushima, L. McLerran, H. Oeschler, R. Pisarski, K. Redlich, C. Sasaki, H. Satz and J. Stachel, Nucl. Phys. A **837**, 65-86 (2010) doi:10.1016/j.nuclphysa.2010.02.005 [arXiv:0911.4806 [hep-ph]].

[12] T. Kojo, Y. Hidaka, L. McLerran and R. D. Pisarski, Nucl. Phys. A **843**, 37-58 (2010) doi:10.1016/j.nuclphysa.2010.05.053 [arXiv:0912.3800 [hep-ph]].

[13] G. Cao, L. He and X. G. Huang, Chin. Phys. C **41**, no. 5, 051001 (2017) doi:10.1088/1674-1137/41/5/051001 [arXiv:1610.06438 [nucl-th]].

[14] J. Steinheimer, S. Schramm and H. Stocker, Phys. Rev. C **84**, 045208 (2011) doi:10.1103/PhysRevC.84.045208 [arXiv:1108.2596 [hep-ph]].

[15] L. McLerran and S. Reddy, Phys. Rev. Lett. **122**, no. 12, 122701 (2019) doi:10.1103/PhysRevLett.122.122701 [arXiv:1811.12503 [nucl-th]].

[16] K. Fukushima and T. Kojo, Astrophys. J. **817**,

no.2, 180 (2016) doi:10.3847/0004-637X/817/2/180 [arXiv:1509.00356 [nucl-th]].

[17] K. S. Jeong, L. McLerran and S. Sen, arXiv:1908.04799 [nucl-th].

[18] S. Sen and N. C. Warrington, [arXiv:2002.11133 [nucl-th]].

[19] D. C. Duarte, S. Hernandez-Ortiz and K. S. Jeong, [arXiv:2003.02362 [nucl-th]].

[20] T. Zhao and J. M. Lattimer, [arXiv:2004.08293 [astro-ph.HE]].

[21] C. J. Xia, S. S. Xue and S. G. Zhou, JPS Conf. Proc. **20**, 011010 (2018) doi:10.7566/JPSCP.20.011010

[22] B. J. Schaefer and J. Wambach, Phys. Rev. D **75**, 085015 (2007) doi:10.1103/PhysRevD.75.085015 [hep-ph/0603256].

[23] J.D. Walecka, Ann. of Phys. 83, 491 (1974).

[24] S. P. Klevansky, "The Nambu-Jona-Lasinio model of quantum chromodynamics," Rev. Mod. Phys. **64**, 649 (1992).

[25] R. Hofstadter, Rev. Mod. Phys., 28:214 (1956).

[26] A. E. S. Green and D. F. Edwards, Phys. Rev., 91:46 (1953).

[27] A. E. S. Green, Phys. Rev., 95:1006 (1954).

[28] S. Shlomo, V. M. Kolomietz, G. Col'o, Eur. Phys. J. A 30, 23-30 (2006).

[29] G. Baym, T. Hatsuda, T. Kojo, P. D. Powell, Y. Song and T. Takatsuka, Rept. Prog. Phys. **81**, no. 5, 056902 (2018) doi:10.1088/1361-6633/aaae14 [arXiv:1707.04966 [astro-ph.HE]].

[30] M. Leonhardt, M. Pospiech, B. Schallmo, J. Braun, C. Drischler, K. Hebeler and A. Schwenk, arXiv:1907.05814 [nucl-th].

[31] P. Danielewicz, R. Lacey and W.G. Lynch, Science 298 (2002) 1592-1596.